Chemosphere 271 (2021) 129426

Contents lists available at ScienceDirect

Chemosphere

journal homepage: www.elsevier.com/locate/chemosphere

Batch and column mode removal of the turquoise blue (TB) over bio-char based adsorbent from *Prosopis Juliflora*: Comparative study

Pamila Ramesh [a, b], Vasanthi Padmanabhan [a, *], R. Arunadevi [c], P.N. Sudha [c, **], Abd El-Zaher M.A. Mustafa [d, e], Abdullah Al-Ghamdi Ahmed [d], Amal H. Alajmi [d], Mohamed Soliman Elshikh [d]

[a] Department of Civil Engineering, School of Infrastructure, B.S.A Crescent Institute of Science & Technology, Vandalur, Chennai, 600048, India
[b] Department of Civil Engineering, Sri Sairam Engineering College, Chennai, 600044, India
[c] PG and Research Department of Chemistry, D.K.M.College for Women, Vellore, 632001, India
[d] Department of Botany and Microbiology, College of Sciences, King Saud University, P.O. Box 22452, Riyadh, 11495, Saudi Arabia
[e] Botany Department, Faculty of Science, Tanta University, Tanta, Egypt

GRAPHICAL ABSTRACT

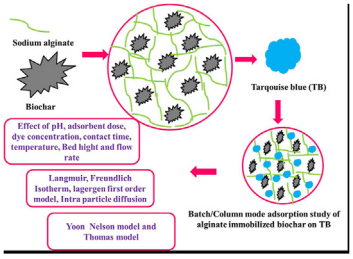

ARTICLE INFO

Article history:
Received 30 October 2020
Received in revised form
15 December 2020
Accepted 21 December 2020
Available online 31 December 2020

Handling Editor: Derek Muir

Keywords:
Biochar
Prosopis Juliflora
Turquoise blue
Adsorption

ABSTRACT

Biochar, created from Prosopis Juliflora (B-PJ) through an ionic polymerization route, was utilized as a sorbent to remediate turquoise blue (TB). The biochar was described utilizing Fourier change infrared spectroscopy. The effects of operating factors such as flow rate, bed depth, concentration, and solution pH were investigated in column mode. Thomas, Yoon-Nelson, and Adams-Bohart models were applied to examine the experimental column data and the correlation between operating factors. The greatest adsorption limit of the BPJ was discovered utilizing 200 mg/L of the adsorbate, B-PJ portion 3 g, at a contact time of 150 min and pH of 6. The adsorption energy and harmony isotherms were all around spoken to by the pseudo-second-request model and the Langmuir model, separately. The most extreme adsorption limit acquired from the Langmuir isotherm model was 0.005173 mg/g. The test energy information dissected utilizing various models featured that the pseudo-second request motor model created a prevalent depiction of the trial information. The adsorption energy followed a pseudo-second-request active model with high connection coefficients (R^2 ›0.98). These outcomes showed that alginate immobilized biochar is earth well-disposed locally accessible, powerful and practical adsorbent for the expulsion of TB color from modern wastewaters.

* Corresponding author.
** Corresponding author.
E-mail addresses: vasanthi_arul@yahoo.com (V. Padmanabhan), drparsu8@gmail.com (P.N. Sudha).

https://doi.org/10.1016/j.chemosphere.2020.129426
0045-6535/

1. Introduction

Ecological contamination issues are expanding alarmingly because of the quick advancement of mechanical exercises. A large portion of the businesses uses colors to shading their items. Material ventures are the significant patrons of ecological contamination because they release hued squander water during their different activities. Because of the high consumption caused by virtue of wastewater treatment, the medium and little scope ventures are giving the wastewater access to the water bodies without legitimate treatment (Markendeya et al., 2015). The wastewater, for the most part, comprises of colors of complex nature, non-biodegradable and poisonous which influences the tasteful appearance, yet in addition, forestalls the passage of daylight into the getting water bodies and henceforth lessens the photosynthetic activity (Rahimi et al., 2013) and furthermore turns into a danger to the human and environment (Pathania et al., 2017). Henceforth decolourization of color effluents has procured expanding consideration during the most recent two decades (Abd El-Latifa et al., 2010). Various traditional strategies are tended to by the analysts for the treatment of color bearing waste water which incorporates physical, concoction and Biological techniques, like coagulation/flocculation, ozonation, adsorption, film filtration, electrolysis, propelled oxidation and particle trade, and so on. Be that as it may, many of the above strategies have certain confinements because of high working cost, the arrival of harmful results and more volume of slop creation (Ayyappan et al.; Singh et al., 2018). Adsorption is one of the physico-synthetic technique, which is seen as the most famous strategy due do its straightforwardness, simple in activity, condition friendly& practical to expel the colors from effluents (Rahimi et al., 2013; Saber et al., 2016; Ates et al., 2020; Said et al., 2020). Adsorption on initiated carbon is the broadest innovation utilized in the evacuation of colors (Markendeya et al., 2015). Adsorption utilizing initiated carbon is seen as increasingly proficient because of numerous focal points, for example, high surface region, remarkable concoction nature of its surface and small scale permeable structure (Abd El-Latifa et al., 2010). Activated carbon is used extensively to expel colors, natural contaminations, and inorganic, for example, metals from the earth (Acemioglu et al., 2019), Until as of late, the customary and broadly utilized carbon-based adsorbent for wastewater treatment has been enacted carbon, however the utilization of actuated carbon has a few detriments, for example, significant expense, issue of recovery (Felista et al., 2020) and arranged from Non-sustainable materials. Notwithstanding, in light of the fact that business initiated carbon is costly and related with an issue of recovery, there is a constant quest for substitute minimal effort, non-traditional, sustainable &green adsorbents by researchers in the ongoing years (Abd El-Latifa et al., 2010; Gokulan et al., 2019). Various kinds of biomaterials have been applied to expel colors and overwhelming metals from squander water because of their minimal effort and improved adsorption potential. Bio sorbents are condition neighbourly as well as promptly accessible in adequate amounts. Since the adsorption capability of numerous biosorbent materials relies on their physico-substance properties and determination of an effective adsorbent is, in this way a prime worry for treatment of color loaded wastewater (Ben Rebah., 2017).

As of late, biochar is considered because of its promising possibilities in different natural applications. Biochar is essentially a rich carbon-comprising stable item acquired from pyrolysis of biomass or different natural inception materials. Biochar is created through a warm separation of natural parts under without O_2 condition (pyrolysis). It has been seen that biochar can remediate different contaminations, for example, supplements, overwhelming metal particles and colors (Contescu et al., 2018). Biochar has been considered a proficient adsorbent practically identical to enacted carbon in the evacuation of natural and inorganic toxicants from mechanical wastewater because of its permeable structure, surface dynamic restricting legends, and huge surface zone (Ben Rebah et al., 2017).

The surface practical gatherings of an adsorbent decide their adsorption conduct and surface reactivity, among different properties. When all is said in done, the last surface functionalities and features are controlled by the enactment procedure and by the idea of burned antecedents. Out of the various kinds of antecedents, lignocellulosic biomass is a promising crude material, as a result of its bountiful accessibility. Aside from the monetary advantages, utilizing this feedstock's for creating bio singes shuts the carbon cycle and aids in taking care of air contamination issues (Yang et al., 2012).

Transformation of rural squanders into biochars cannot exclusively spare regular assets yet in addition ensure condition against environmental change (22). For the most part, biochar quality is impacted by its feedstock type just as pyrolysis circumstances (Xie et al., 2015). Biochar is a transcendently steady, stubborn natural carbon (C) compound made when biomass (feedstock) is warmed to temperatures generally somewhere in the range between 300 and 1000 °C, under low (ideally zero) oxygen fixations. Biochar is a piece of a progression of materials alluded to as dark carbons, which are completely created by a substance as well as a warm change of the first biomass material (Gokul et al., 2017). Alongside the horticultural waste base adsorbent, sodium alginate-based composite also saw as valuable for the expulsion of color from its watery arrangement (Li et al., 2013; Hassan et al., 2014; Benhouria et al., 2015). Characteristic polysaccharide acquired from earthy colored green growth is termed as alginate. Because of its accessibility and simple extraction process alginate are minimal effort material (Benhouria et al., 2015). The fluid arrangement of alginate is thick and gooey, and within sight of a divalent cation, it shapes a hydrogel by composition component. This hydrogel arrangement is recognized as inotropic gelation. Utilizing this features of gel development of alginate, actuated carbon, mud and nanomaterials can be ensnared in the alginate gel and employed for adsorption activity.

Alginate is a minimal effort material owing to its accessibility and easy extraction process (Benhouria et al., 2015). The alginate fluid arrangement is dense and gooey, and it forms a hydrogel by composition variable within sight of a divalent cation. This arrangement with hydrogel is labelled as inotropic gelation. Using this gel creation property, alginate, actuated carbon, mud and nanomaterials can be ensnared in the alginate gel and added to the activity of adsorption. The proximity of various people often differs. In addition, the proximity of numerous utilitarian groups in the alginate gel, such as COO, OH, CH], and so on, increase the cation's uptake.

From the most recent quite a long while, in genuine thought of the overall financial and natural contamination issues, there has been expanding research enthusiasm for estimating bio-sourced lignocellulosic biomass as a valuable adsorbent for wastewater treatment for evacuating natural color. Biomass contained on lignocellulosic squander is an economical, inexhaustible, uninhibitedly accessible in plentiful and gives a one of a kind normal asset to the enormous scope and practical bio-vitality assortment.

Prosopis Juliflora (Mesquite) picked for planning Bio burn in this current examination, is a sort of Invasive plant species. This prickly bush seriously affects groundwater as it exhausts the degree of water since it tends to assimilate groundwater and in its water by engrossing it from environmental dampness. No other plant species can coincide with Prosopis Juliflora (Lagergren et al., 1898).

A public interest writ petition that was filed a few months ago in

the Madras High Court directing the government to immediately launch a campaign for the mechanical removal of *Prosopis Juliflora* from all public spaces, hence this paper aims for finding ways to gainfully utilize it. This study aims to prepare a novel bio-char based adsorbent from *Prosopis Juliflora* [Mesquite] to be applied as biosorbent for the elimination of reactive turquoise blue (TB) dye from aqueous solutions. The dynamic conduct of fixed-bed section was portrayed as far as the advancement bend. As a component of this examination, the impacts of bed profundity, stream rate, and starting feed focus on TB adsorption execution onto alginate immobilized biochar were researched. Various models, for example, Thomas, Yoon-Nelson, and Adams-Bohart models were utilized to examine the test information.

2. Materials and methods

2.1. Reagents and solutions

TB cationic dye was received from Merck. All the chemicals used were of analytical quality acquired from Merck chemicals, India.

2.2. Preparation of acid activated BioChar

18 N sulfuric acid was taken, in which the biochar was immersed for 2 h. Double distilled (DI) water was applied to wash the carbonized material until the pH reached neutral. The biochar was dried in a hot air oven at 393 K. Subsequently, the obtained carbonized material was subjected to a muffle furnace at 723 K for 3 h for complete carbonization. The carbon was ground and sieved into 180–300 μm standard sieves by a mechanical sieve.

2.3. The activated bio char/Calcium alginate polymer bead preparation

Ionic polymerization method was used to prepare the composite beads. 1.2 g of sodium alginate powder was added to 100 mL of boiled DI water, taken in a beaker, and stirred for 2 h till a gelatinous solution was attained. Afterward, 1.2 g of carbon was introduced and agitated for 1 h. The prepared mixture of carbon in gelatinous alginate was added drop by drop to 0.2 mol kg^{-1} of $CaCl_2$ solution. Then the obtained aqueous drops get gelled into polymeric beads when they contact with the $CaCl_2$ solution. The subsequent polymer beads were finally washed with DI water several times to eliminate excess $CaCl_2$ (Kumar et al., 2013).

2.4. Batch sorption studies

50 mL of TB solution was taken in a conical flask and was shaken in an orbit shaker at 140 rpm for doing batch experiments. 0.25 g–3 g of alginate immobilized biochar was applied to inspect the effect of adsorbent dosage on the adsorption efficacy. The experiment was conducted at room temperature. The effect of initial dye concentration was assessed by changing the TB concentration varying from 4 to 200 mg/L. Also, the temperature effect was studied at a temperature ranging from 30 to 50 °C, while pH was examined by altering the TB dye pH from 3 to 12. Aliquots were withdrawn and the absorbance was evaluated via a UV-VIS spectrophotometer.

2.5. Column experiments

The effect of flow rate, bed height, and inlet concentration on the breakthrough curves was studied using UV adsorption performance.

2.5.1. Effect of flow rate

The foreordained stream rates were changed under 1, 2 and 3 mL/min to examine its impact on the adsorption execution. The bed stature and bay fixation were kept steady at 2 cm and 200 ppm, individually.

2.5.2. Effect of bed height

The predetermined bed heights maintained were 1, 2 and 3 cm to inspect the influence on the adsorption features.

2.5.3. Effect of initial dye concentration

The predetermined initial inlet concentrations were 100, 200, and 300 ppm to observe the effect on the adsorption features. The bed height and flow rate factors were kept constant at 2 cm and 3 mL/min correspondingly.

2.6. Dye analysis

The centralization of TB staying in the supernatant after and before sorption was resolved with a 1.0 cm light way quartz cells utilizing UV–Vis twofold pillar spectrophotometer, at λ_{max} of 490 nm. The adsorbed color sum (mg/g), qt and the rate expulsion of color whenever were registered as follows, individually:

$$qt = (C_0 - C_1)\,(V / M) \tag{1}$$

$$\%\ removal = [(C_0 - C_t) / C_0].100 \tag{2}$$

where C_0 and C_t are the initial and concentration of dye at certain periods (mg/L), V is the volume of the solution (L) and M is the adsorbent mass (g).

2.7. Isotherm and kinetic studies

The isotherm conditions utilized in this examination are Freundlich and Langmuir isotherm conditions of straight and non-direct relapse techniques. In Langmuir isotherm, different types of linearized conditions were analyzed. The dynamic examination helps for the forecast of sort of components required during the sorption procedure. So as to get dynamic information of the adsorption procedure, Lagegren's pseudo-1st request and pseudo-2nd request motor conditions were utilized. Biosorption energy tests were completed in 250 mL jars having 50 mL of the color arrangements utilizing a known measure of nut husk. The jars were upset for different time stretches (0–180 min) on an orbital shaker. The examples were taken at various periods, centrifuged and investigated for residual color fixations as portrayed previously. The motor information was analyzed utilizing pseudo-1st request (Ho et al., 2000), pseudo-second request (Weber et al., 1963) and intraparticle dispersion (Nasrullah et al., 2018) dynamic models.

2.8. Yoon and Nelson model

Yoon and Nelson model capacities dependent on the hypothesis that a decline in the pace of adsorption likelihood for each adsorbate atom is directly related to the likelihood of adsorbate adsorption and advancement onto the adsorbent. Also, this model is less mind-boggling than others as it doesn't require subtleties of adsorbate attributes, the kind of adsorbent, and the physical features of the adsorption. This model comprises of $C_t/(C_0 - C_t)$ vs. sampling time (t) as displayed in Eq. (3).

$$C_t / C_o - C_t = \exp(k_{YN}t - \tau k_{YN}) \tag{3}$$

The nonlinear regressive model was employed to obtain

parameters k_{YN} and τ.

2.9. Thomas model

Thomas model is applied to govern the supreme ability of an adsorbent. The maximal solid-phase concentration of the adsorbate, TB dye, onto the adsorbent and adsorption rate constant was dogged using a Thomas kinetic model. The Thomas model is expressed in Eq. (4).

$$\ln(Co/Ci - 1) = kTh_{qow}/Q - k_{Th}C_o t \quad (4)$$

Where k_{Th} signifies Thomas constant (ml min^{-1} mg^{-1}), q_o is the equilibrium adsorption quantity of dye, TB on adsorbent (mg g^{-1}), w is the mass of the adsorbent (g) and Q is the flow rate (ml min^{-1}).

2.10. Characterization of biochar-alginate nanocomposites

FT-IR estimations of the readied alginate immobilized biochar adsorbate were logged via Fourier Transform Infrared Spectrophotometer (FT-IR) utilizing the PerkinElmer 200.

3. Result and discussion

3.1. FT-IR

The FT-IR spectra were utilized to decide the nearness of different practical gatherings present in crude biochar and alginate immobilized biochar. Fig. 1a displays the FTIR spectra of crude biochar and Fig. 1b delineates the FTIR spectra for alginate immobilized biochar. Top at 995 cm^{-1} means that the nearness of beta glycosidic bond. This locale speaks to the total of the vibration of valence groups of the hydrogen obligation of the OH gathering and the groups of the intra-atomic and intermolecular hydrogen bond. Tops at 2362 cm^{-1} sign the nearness of symmetric CH and CH_2, and top about 2922 speak to the uneven CH and CH_2. The nearness of OH bunch is identified from the tops over 3398 cm^{-1} (Alencer et al., 2012).

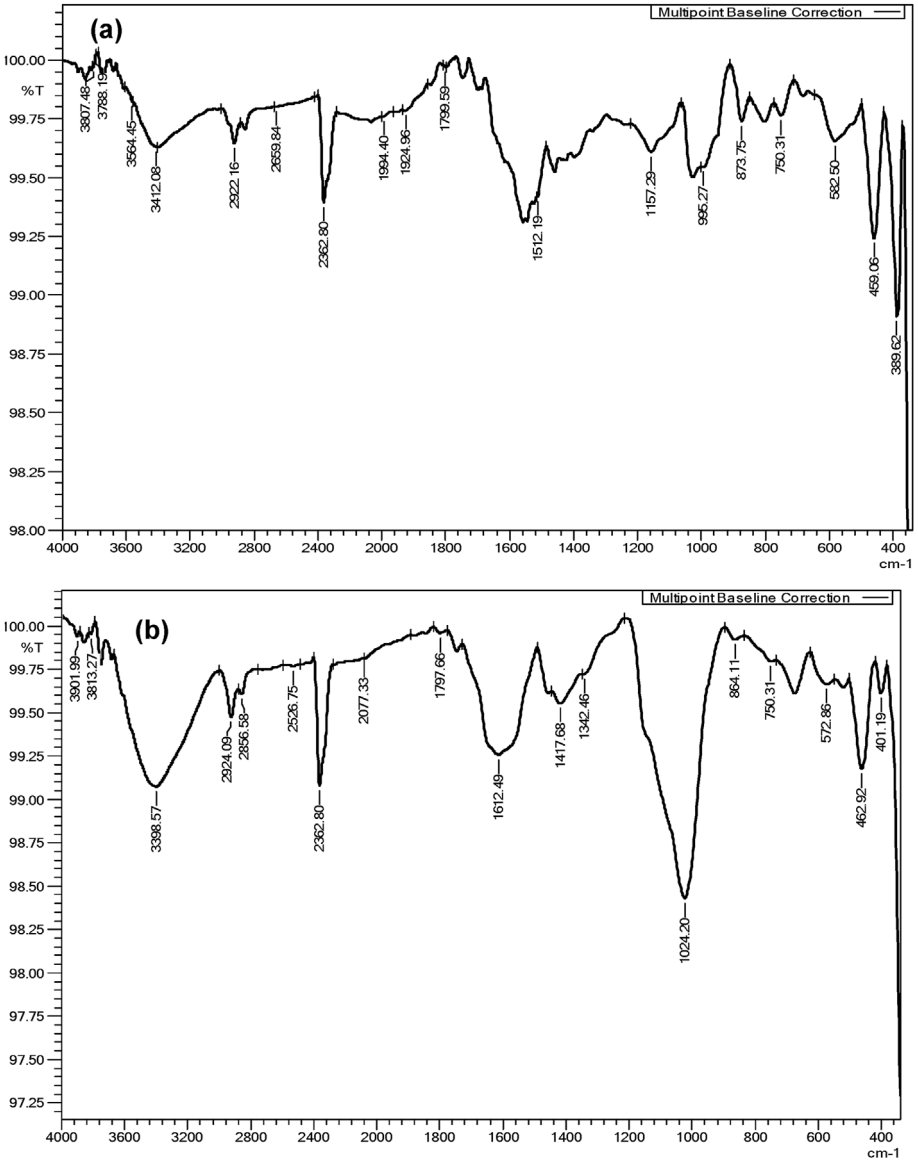

Fig. 1. FTIR Spectrum of a) biochar b) alginate immobilized biochar.

3.2. Batch and column mode adsorption results by biochar and alginate composite adsorbents

The adsorption examination of TB dye over the B-PJ was carried out in batch and column operation modes. In batch mode, kinetic and equilibrium evaluations were performed. After then, column flow mode studies were initiated. In order to decide the ideal operational boundaries overseeing the adsorption cycle, the impact of pH, adsorbent portion, beginning color focus and impact of temperature were researched.

3.2.1. Batch adsorption studies

3.2.1.1. Effect of pH. One of the most significant variables affecting the adsorption of color on an adsorbent is the adsorbate arrangement's pH (Safa et al., 2011). pH influences the accessibility of color atoms and furthermore impacts the exercises of practical gatherings on the adsorbent surface. Analyses were led to look at the impact of pH on the adsorption of TB color by differing the pH from 3 to 12. The outcomes showed that the most extreme color evacuation is accomplished at pH 6 and an increment in pH brings about diminished adsorption of color (Fig. 2a). This is because of the way that at lower pH the adsorbent surface achieves the positive charge and solid electrostatic fascination between the decidedly charged adsorbent surface and color anions prompts the higher color expulsion from watery arrangements (Salleh et al., 2011). The diminished adsorption at high pH can likewise be clarified as at antacid pH nearness of abundance OH-particles destabilize the color anions and rival the color anions for the adsorption locales (Savova et al., 2003). The outcomes are likewise affirmed by the pHPZC of Alginate immobilized Biochar as beneath this pH adsorbent surface conveys positive charge and upgrades the expulsion of anionic colors (Namasivayam et al., 1988).

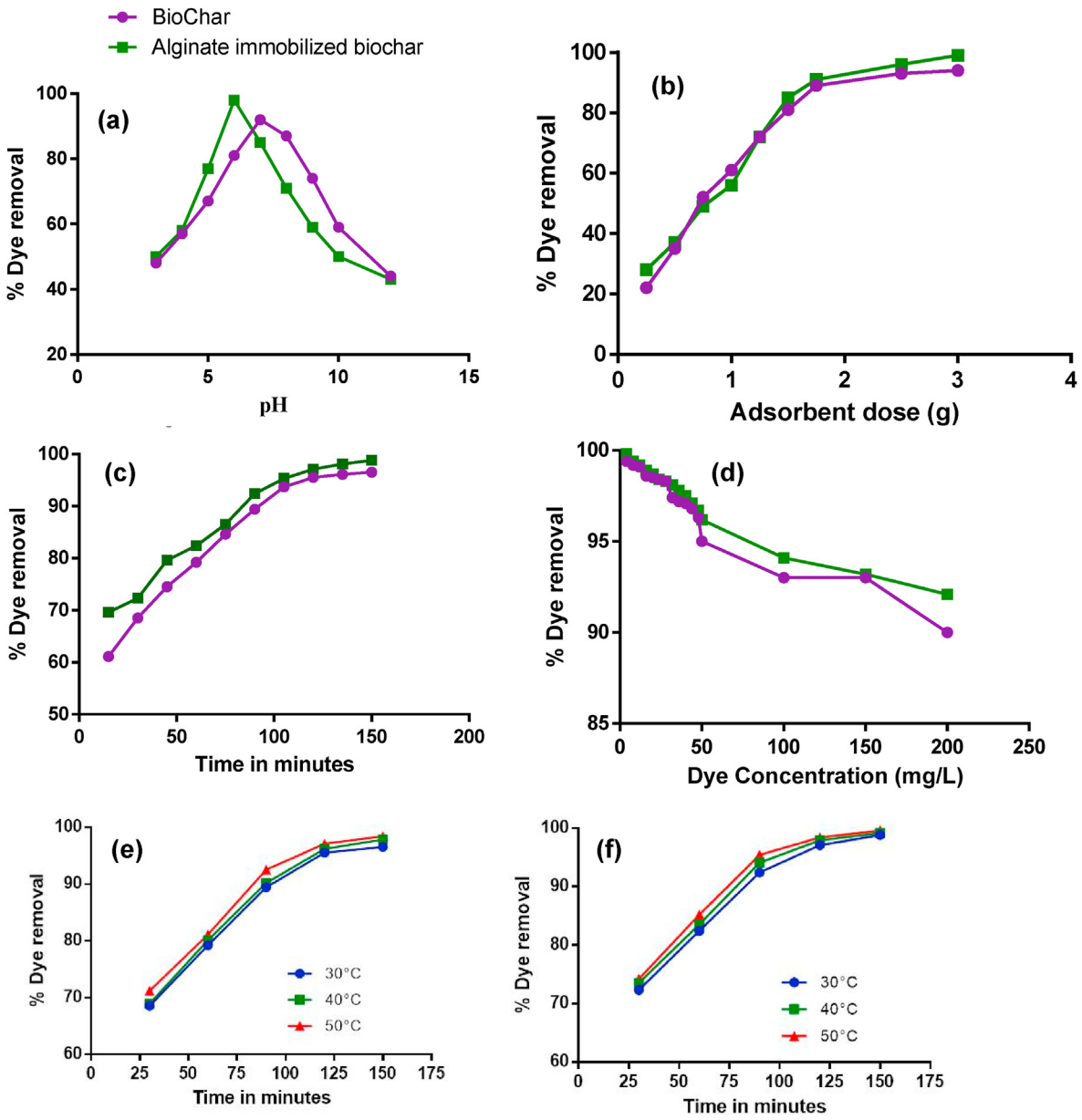

Fig. 2. Batch absorption studies. Effect of pH (a), adsorbent dosage (b), contact time (c), initial dye concentration (d) studies on Biochar and Alginate immobilized Biochar; Effect of temperature studies on (e) Biochar (f) Alginate immobilized Biochar on TB.

3.2.1.2. Effect of adsorbent dosage. The most elevated watched color expulsion efficiencies for both biochar and alginate immobilized biochar were at 3 g. This was likely because of the total, which was unmistakably obvious at higher biochar fixations. Despite this decline in expulsion proficiency, expanding the adsorbent focus resulted in an expanded level of the all-out overwhelming metals expelled (Fig. 2b). Alginate immobilized biochar was concentrated by fluctuating various adsorbents from 0.25 to 3 g while keeping different boundaries, for example, pH (6), contact time, temperature and introductory metal particle focus (200 mg/L) as steady. Notably, it is obvious that the adsorption of TB upsurges quickly with the expansion of adsorbent from the start; however, it stays consistent in the wake of arriving at an ideal measurement. The fast take-up uncovered a high liking between the adsorbent and the adsorbate, which was legitimately ascribed to the adsorbent's characters. In any case, further expansion of the adsorbent past 3 g in the two cases didn't provide any substantial modification in the adsorption owing to the congestion of adsorbent particles (Gokila et al., 2017; Kannan et al., 2001). On looking at the adsorbent portion, it demonstrated that at the dose of 3 g, the most extreme adsorption in the alginate immobilized biochar is seen at 99%. Any further expansion of the adsorbent past this didn't bring about any critical change in the adsorption. Notably, the observed phenomenon evidences the covering of adsorption locales because of the congestion of adsorbent particles.

3.2.1.3. Effect of contact time. The impact of contact time dictated by utilizing starting convergence of TB is 50 200 mg/L, adsorbent portion is 3 g/250 mL and pH is 6 at 30 °C with various time span, for example, 15, 30, 45, 60, 75, 90, 105, 120, 135 and 150 min as appeared in Fig. 2c. The % evacuation of TB expands at first and arrives at practically consistent worth. So the ideal contact time for the TB adsorption was taken as 150 min.

3.2.1.4. Effect of initial dye concentration. The initial dye concentration has a noticeable influence on its elimination from aqueous solutions. The adsorption of TB on biochar and alginate immobilized biochar was examined as a component of contact time at the distinctive introductory TB focuses on the scope of 0–150 min at room temperature. It was discovered that the evacuation of color by biochar diminished from 99.4% to 90% with expanding starting grouping of TB from 4 to 200 mg/L, and the expulsion of color by alginate immobilized biochar diminished from 99.8% to 92% with expanding introductory convergence of TB from 4 to 200 mg/L. Thusly, the adsorption rate diminishes and the degree of adsorption increment with diminishing beginning TB focus. This shows a decrease in prompt solute adsorption, attributable to the absence of accessible dynamic locales mandatory for the high beginning centralization of TB. In contrast, the genuine measure of color adsorbed per unit mass of biochar and alginate immobilized biochar expanded with the expanded in introductory fixation as introduced in Fig. 2d. This expansion is because of the lessening in protection from the take-up of solute from color arrangement. Comparative outcomes have been accounted for in writing (Cicek et al., 2007; Langmuir et al., 1918). At long last, it very well may be seen from Fig. 2d that alginate immobilized biochar has the most extreme rate evacuation contrasted with biochar.

3.2.1.5. Effect of temperature. For the most part, the color evacuation efficiencies expanded with the expansion of temperature and afterward kept steady (Fig. 2e and **f**). The degree of adsorption relies upon the temperature of the strong fluid interface. Thermodynamic boundaries and active procedure relied upon the structure of TB and surface useful gatherings of an adsorbent. The impact of temperature was learned at 30, 40 and 50 °C and the outcomes were summed up in Fig. 2e and **f**. The results show that the % evacuation of TB color in the 200 mg/L scopes diminishes with the temperature rise.

Table 1
Mathematical model of Langmuir and freundlich Isotherm values.

Mathematical Models	Parameters	Biochar	Alginate immobilized biochar
Langmuir Isotherm	$K_L(dm^3/g)$	51.57	62.3
	$b(dm^3/g)$	0.001366	0.005173
	$C_{max}(mg/g)$	0.005171	0.005173
	R^2	0.8730	0.8671
Freundlich Isotherm	K_F	0.1901	0.2030
	N	1.8498	1.9763
	1/n	0.5406	0.506
	R^2	0.9904	0.9944

3.2.2. Adsorption isotherm

The Freundlich and Langmuir models were utilized to fit with test information and these boundaries are appeared in Table 1. Langmiur and freundlich models were utilized to explore the harmony conduct of TB adsorption on the readied biochar and alginate immobilized biochar. Langmuir isotherm, which accepts that there is a limited number of restricting destinations appropriated homogeneously over the outside of the adsorbent can be spoken to as

$$\frac{Ce}{qe} = \frac{1}{Qb} + \frac{Ce}{Q0} \tag{5}$$

Where C_e is harmony fixation (mg^{-1}) qe is a measure of TB adsorbent at balance (mg/g) are Langmuir constants. Indicating the immersed monolayer adsorption limit and sorption harmony consistent, individually (Zhang et al., 2012).

A plot of Ce and Ce/qe ought to speak to a line with slant of and capture of and individual information are introduced in Table 1. The higher relationship ($R^2 > 0.9944$) coefficient flexibly and the possibility for best portrayal of balance information compare to Langmuir isotherms of biochar and TB adsorption on to alginate immobilized biochar over entire focus extend greatest monolayer adsorption limit of 0.005173 mgg^{-1}.

From the Freundlich adsorption limits esteem increments with raise in temperature; this was expected to multilayer adsorption.

$$\log g_{e=} \log K_F + logC_e \tag{6}$$

Where K_F and n speak to the harmony constants demonstrate the adsorption limit and adsorption power, separately (if $n > 1$, the adsorption is viewed as good) (Plazinslic et al., 2010). The qualities for consistent K_F were acquired from slant and estimation of the log qe versus log Ce and are recorded in Table 1. The adsorption force can likewise be communicated as far as n esteems. The n esteems between 1 and 10 show the adsorption was positive. The n esteems determined from Freundlich isotherm was likewise lying in the middle of 1–10. This demonstrates the Freundlich adsorption was an ideal procedure. Adsorption limits of these two isotherms demonstrate that the adsorption was a physical adsorption. From the figure it shows the Freundlich (Fig. 3a and b) and Langmuir (Fig. 3c and d) boundaries, wherein coefficient relationship esteems (r^2) of Langmuir isotherm was closer to 1 than of Freundlich isotherm. Along these lines, the Langmuir isotherm was more followed than the Freundlich isotherm.

3.2.3. Adsorption kinetics

The lagergen-1st order model (Ofomaja et al., 2010; Tseng et al., 2003; Ho et al., 1998; Ho et al., 2003; Ho et al., 2001; Wu et al., 2002; Weber et al., 1963a, b) can be illustrated as

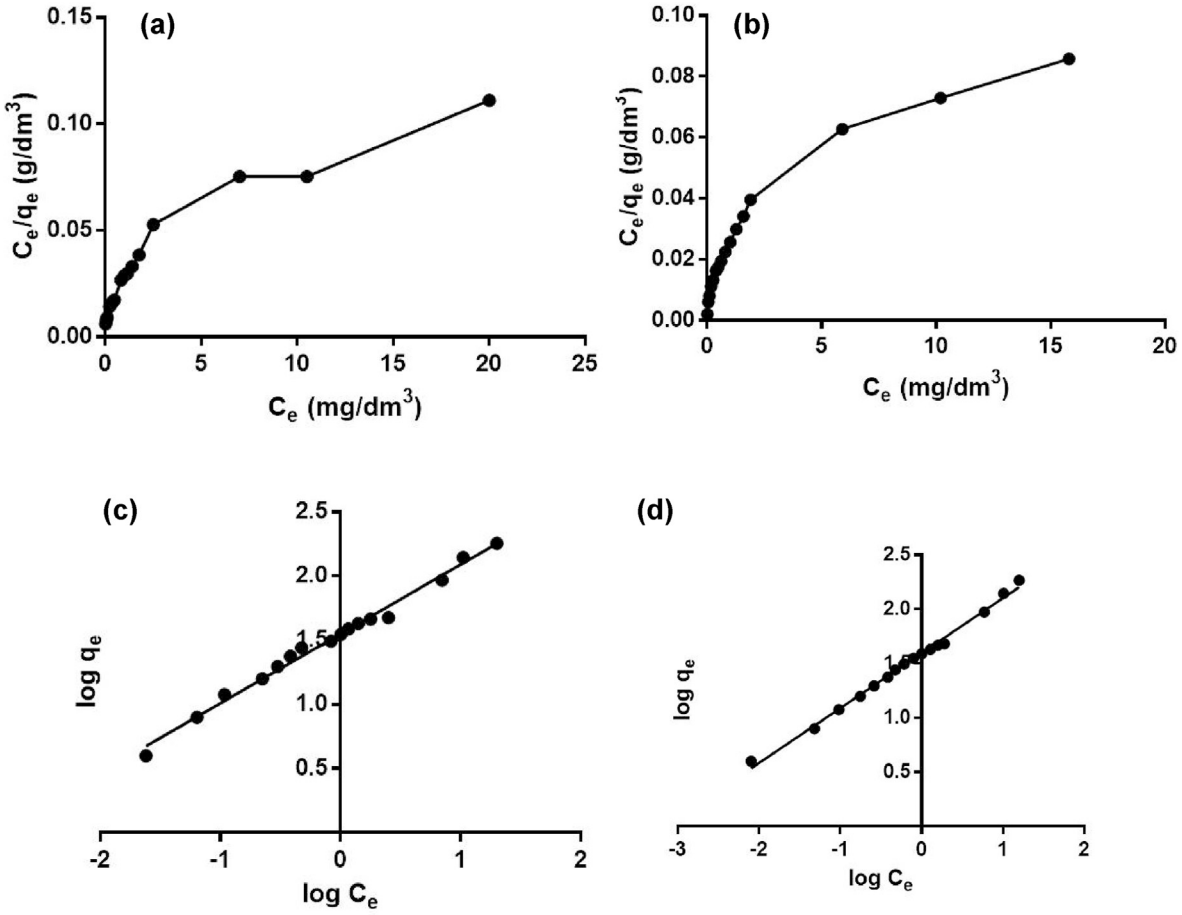

Fig. 3. Langmuir adsorption isotherm of a) Biochar b) Alginate immobilized biochar and Freundlich adsorption isotherm c) Biochar d) Alginate immobilized biochar.

$$\log(Q_e - Q_t) = \log Q_1 - \frac{K_1}{2.303}t \tag{7}$$

The pseudo-second-order model (Zhang et al., 2012) can be expressed as

$$\frac{t}{Q_t} = \frac{1}{K_2 Q_2^2} + \frac{t}{Q_2} \tag{8}$$

Q_e and Q_t are the amount of TB adsorbed on the adsorbent at equilibrium. At the various time (mg/g), Q_1 and Q_2 are the Lagergren 1st-order model's calculated adsorption capacities and the pseudo-2nd-order model (mg/g). K_1 and K_2 the rate constant of the Lagergren 1st-order model (min^{-1}) and the pseudo-2nd-order model (g/(mg.min)). The correlation coefficients R^2 for the pseudo-2nd-order adsorption model have the maximum values (>0.99), signifying that the dye adsorption process is mostly ruled via the pseudo-2nd -order adsorption mechanism. Fig. S1 and Fig. S2 shows the pseudo-1st and 2nd order kinetics of biochar and alginate immobilized biochar respectively, respectively, and are recorded in Table 2.

3.2.4. Intraparticle diffusion model

The general pace of the sorption procedure will be constrained by the slowest, the rate restricting advance. The idea of the rate-restricting advance in a cluster framework can be resolved from the solute and sorbent properties. In adsorption frameworks where there is the chance of intraparticle dispersion being the rate-constraining advance, the intraparticle dissemination approach depicted by Weber and Morris (Weber et al., 1963a, b) is utilized. The rate constants for intraparticle dispersion (ki) are resolved utilizing the condition given by Weber and Morris. This condition can be portrayed as (Jain et al., 2002; Weber et al., 1963a, b; Sivaraj et al., 2001; Markovska et al., 2001; Biswas et al., 2019):

$$q_t = k_i t^{0.5} + c \tag{9}$$

where k_i and c are the intraparticle diffusion rate constants under numerous initial concentrations of dye and a constant, correspondingly. In Fig. S3, shows $t^{1/2}$ vs qt plots for biochar and alginate immobilized biochar (Table 2).

3.2.5. Column adsorption studies

The effect of bed height, flow rate and initial inlet concentration onto the breakthrough curve shape by means of column performance had been assessed.

3.2.5.1. Effect of adsorbent bead bed height. The bed tallness or the adsorbent stacking is another significant boundaries in structuring any stuffed bed, fluidized bed or semi fluidized bed adsorption reactor. The fixation profile concerning the time at various bed statures was gotten for TB adsorption at a steady stream rate and starting focus (100 mg/L) has appeared in Fig. 4. It very well may be considered that to be bed tallness expands; the measure of adsorbent and dynamic help region builds, which brings about better expulsion effectiveness of TB from the arrangement. It has been

Table 2
Mathematical models of kinetics and intraparticle diffusion values.

Mathematical Models	Parameters	BioChar	Alginate immobilized biochar
Pseudo first order	q_e(mg/g)	0.3677	0.3375
	k_1(min^{-1})	0.0366	0.0306
	R^2	0.9145	0.9264
Pseudo second order	q_e(mg/g)	215.05	214.91
	k_2(g $mg^{-1}min^{-1}$)	2.7×10^{-4}	3.28×10^{-4}
	R^2	0.9958	0.9959
Intra particle diffusion	k_{id}	9.114	7.810
	C	88.51	106.5
	R^2	0.9798	0.9776

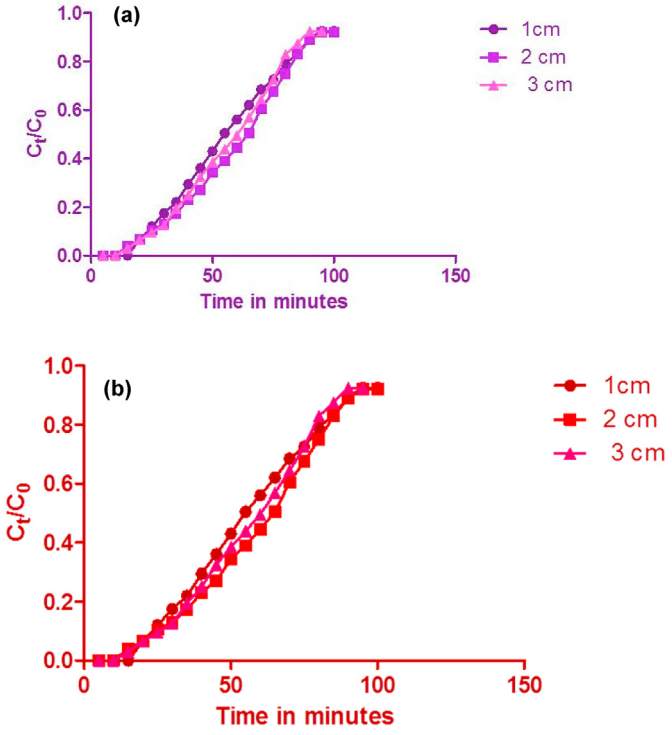

Fig. 4. Effect of bed height a) biochar b) alginate immobilized biochar.

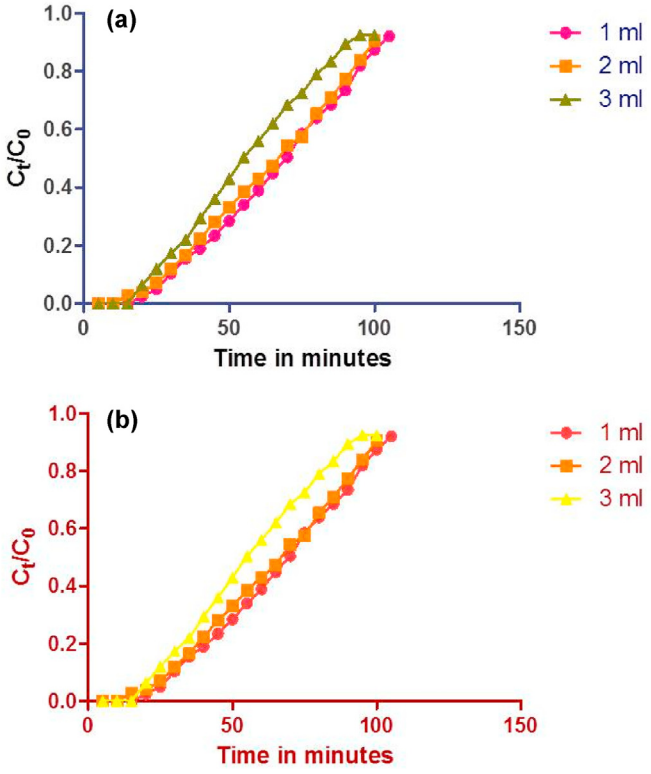

Fig. 5. Effect of flow rate a) biochar b) alginate immobilized biochar.

apparent from the fixation profile that, for higher bed stature or more measure of adsorbent present in the segment, the bed life is greater and the framework arrives at balance quickly. This marvel can be clarified from a mass exchange perspective too. At higher bed stature, the solute gets increasingly dynamic destinations and more communication time for official and less rivalry between the adsorbate atoms, improving rate adsorption. With an increment in bed stature, pressed bed development propensity increments (Singha et al., 2015) in a semi-fluidized bed, diminishing the pivotal scattering coefficient and improving the dispersion of TB color in the adsorbent. So higher bed stature brings about a diminishing in outlet focus over a similar period for example lower advancement time. Besides, enacted carbon stacking is additionally higher at higher beginning adsorbate fixation. Higher take-up was seen with higher bed tallness because of the expansion in the surface zone of the adsorbent accessible per unit mass of TB.

3.2.5.2. Effect of solute flow rate. The impact of different flow rate (1, 2 and 3 mL/min) advancement bends was examined whereby bed stature of 2 cm and an underlying gulf centralization of TB of 100 mg/L are kept steady. The outcomes got are shown in Fig. 5a and **b** and Table S1. The advancement happens quicker at a higher stream rate. The most elevated expulsion level of TB, 92.20% was gotten at least stream pace of 2 mL/min and the test adsorption limit of TB was around 100 mg/g. The stream rate was conversely corresponding to advancement time. As the stream rate builds, a decline in advancement time was obviously watched. At a higher stream rate, the pace of mass exchange increments as the measure of color adsorbed onto unit bed stature is expanded with expanding stream rate driving towards quicker immersion in a flash (Vijayaraghavan et al., 2005).

3.2.5.3. Effect of initial dye concentration. Endeavors were likewise had to explore the effect of beginning TB fixation on remediation of TB in fixed section. For this reason, beginning TB focuses have fluctuated from 100 to 300 ppm at fixed stream rate and biochar bed profundity. Table S1 sums up significant section boundaries saw at various TB focuses. The advancement bends as saw by shifting the underlying TB fixations are introduced in Fig. 6. The most minimal beginning TB fixation created a late advancement bend, inferable from the nearness of overabundance restricting

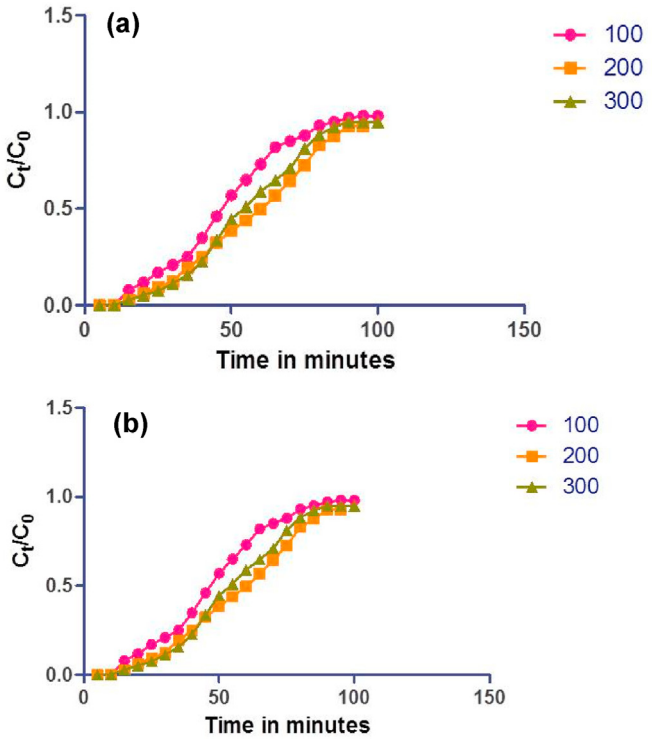

Fig. 6. Effect of initial concentration a) biochar b) alginate immobilized biochar.

locales contrasted with size of color particles (lower focus angle) (Han et al., 2009).

3.2.6. Yoon and Nelson model

To analyse the breakthrough features of TB dye on alginate immobilized biochar packed in the column, the Yoon and Nelson model was introduced. Table S2 lists the rate constant, kYN and time needed to achieve 50 percent of the TB breakthrough, acquired through experiment. Initially, with the upsurge in inlet concentration of TB dye, the rate constant values decrease by kYN. Meanwhile, as the flow rate of the TB dye increases, kYN was witnessed as the rate of constant values increased. The ζ values obtained suggest an upward trend with a rise in the initial TB dye inlet concentration. Besides, the obtained values ndicate a downward trend with a rise in the TB dye flow rate. The value of ζ upsurges and the constant value of k_{YN} decreases as the bed's height increases. Fig. S4 and S5 demonstrates the contrast of the experimental curve and the projected curves employing the Yoon and Nelson model. The experimental breakthrough plots were incompatible with the Yoon-Nelson model curve that was expected. Thus, using the Yoon-Nelson model, a large deviation was found between the observed and expected values.

3.2.7. Thomas model

Using the Thomas model's linearized version, ln (C_o/C_i-1) versus t map, the rate constant, k_{Th}, and qo values were calculated. Table S3 presents the Thomas parameters and linear regression coefficients (R^2) obtained from various experimental parameters. Comparing the experimental results with the expected breakthrough curves at an initial inlet concentration of 200 ppm is displayed in Fig. S6 and S7. As the flow rate and bed height rise, the obtained values of k_{Th} and q_o increase. Reduction in both q_o and k_{Th} values has been achieved as the initial inlet concentration of TB dye increases. Thomas model shows some strong changes with adsorption circumstances based on comparing the experimental curve and projected curves obtained, albeit given with weak correlation. Further, clear differences were found between the experimentally obtained and measured adsorption capability values with the m.

Generally, the Thomas model is used in the fixed bed column to describe the biosorption process's action. Though, this model has some drawbacks in that the derivation is built on 2nd-order kinetics and implies that the chemical reaction does not restrict biosorption, but is calculated at the interface by mass transfer (Aksu et al., 2004; Xie et al., 2015). The Adam Bohart model (Fig. S8 and **S9**) postulates that the decrease in sorbate sorption rate is equally proportionate to both the probability of sorbate adsorption and the likelihood of a breakthrough in the column. At different initial TB concentrations, the two constants (k_{Th} and Q_0) of the Thomas model, the Yoon Nelson model and the Adam Bohart model were determined; solvent flow rates and bed height are shown in Table S2 to S4.

3.2.8. Comparison with other adsorbents and adsorbates

The estimations of the TB limits in adsorption strategy were thought about in Table S5. Numerous analysts have inspected the proficiency of different ease adsorbents in section and cluster mode to eliminate TB. Correlations of various adsorbents found in the writing were done dependent on adsorption limit. From the examination, Alginate immobilized biochar can be viewed as a significant option for eliminating TB from an aqueous solution.

3.2.9. Reusability of the adsorbent

Reusability of adsorbent has a significant essentialness in the conservative and natural perspectives. Reusability of the adsorbent was finished by rehashing the adsorption-desorption cycle multiple times. For the recovery of alginate immobilized biochar, customary techniques like warm actuation, cremation, and land removal were not used to confine ecological contamination. Recovery was finished by 0.1 M HCl arrangement and the test was rehashed for three adsorption-desorption cycles. In first cycle 95.2% evacuation was accomplished and in the third cycle, the expulsion proficiency of 90.4% was accomplished (Fig. S10). Expulsion effectiveness diminishes as cycle continues on the grounds that the utilization of corrosive arrangement may obliterate the coupling locales of the biochar impetus, or deficient corrosive arrangement may permit the TB to stay in the coupling destinations.

4. Conclusion

The study evidences that the removal of TB using alginate immobilized biochar is an effective and feasible method. Langmuir and Freundlich isotherm models were tried in the cluster method of study. As per the outcomes, Langmuir is an increasingly great isotherm model than the others. At higher temperatures, the exothermic idea of adsorption process and the powerless bonds between color particles and restricting locales of alginate immobilized biochar can clarify this circumstance. The cluster dynamic examination demonstrated that the adsorption of TB color on to alginate immobilized biochar could be well fitted by the pseudo-2nd-request condition. Adsorption capacities were higher at the flow rate of 3 mL/min, bed depth of 2 cm, influent concentration of 100 mg/L, and pH of 6. Both of the Yoon Nelson, Thomas and Adam Bohart models created adequate outcomes for structuring an adsorption section. As per the after-effects of cluster and segment examination, evacuation paces of TB color is higher in clump mode adsorption. Moreover, scientific displaying of the adsorption dynamic under constant stream conditions could significantly limit genuine applications.

Declaration of competing interest

The authors declare that they have no known competing financial interests or personal relationships that could have appeared to influence the work reported in this paper.

Acknowledgments

All authors are grateful to the Deanship of Scientific Research at King Saud University Saudi Arabia for financial support through project No RG-1441-484. Authors Pamila and Vasanthi Padmanabhan acknowledge the support provided by B.S.A Crescent Institute of Science & Technology

Appendix A. Supplementary data

Supplementary data to this article can be found online at https://doi.org/10.1016/j.chemosphere.2020.129426.

Credit to author statement

All the authors take credit for the performance of the manuscript and drafting the manuscript.

References

Abd El-Latifa, M.M., Ibrahim, A.M., 2010. Removal of reactive dye from aqueous solutions by adsorption onto activated carbons prepared from oak sawdust. Desalination and Water Treatment 20, 102–113.
Acemioğlu, B., 2019. Removal of a reactive dye using NaOH-activated biochar prepared from peanut shell by pyrolysis process. Int. J. Coal. Preparation. Utilization. 1–23.
Aksu, Z., Gönen, F., 2004. Biosorption of phenol by immobilized activated sludge in a continuous packed bed: prediction of breakthrough curves. Process Biochem. 39 (5), 599–613.
Alencar, W.S., Acayanka, E., Lima, E.C., Royer, B., De Souza, F.E., Lameira, J., 2012. Application of Mangifera indica (mango) seeds as a biosorbent for removal of Victazol Orange 3R dye from aqueous solution and study of the biosorption mechanism. Chem. Eng. J. 209, 577–588.
Ates, A., Oymak, T., 2020. Characterization of persimmon fruit peel and its biochar for removal of methylene blue from aqueous solutions: thermodynamic, kinetic and isotherm studies. Int. J. Phytoremediation 22, 607–616.
Benhouria, A., Islam, M.A., Zaghouane-Boudiaf, H., Boutahala, M., Hameed, B.H., 2015. Calcium alginate-bentonite-activated carbon composite beads as highly effective adsorbent for methylene blue. Chem. Eng. J. 270, 621–630.
Biswas, S., Sen, T.K., Meikap, B.C., 2019. Experimental hydrodynamic and bed characteristics of co-current gas-liquid-solid three phase semifluidization with liquid as the continuous phase. Part. Sci. Technol. 1–13.
Cicek, F., Ozer, D., Ozer, A., 2007. Low cost removal of reactive dyes using wheat bran. J. Hazard Mater. 146, 408–416.
Contescu, C.I., Adhikari, S.P., Gallego, N.C., Evans, N.D., Biss, B.E., 2018. Activated carbons derived from high-temperature pyrolysis of lignocellulosic biomass. C—J. Carbon. Research. 4, 51.
Felista, M.M., Wanyonyi, W.C., Ongera, G., 2020. Adsorption of anionic dye (reactive black 5) using macadamia seed husks: kinetics and equilibrium studies. Scientific African 7, e00283.
Gokila, S., Gomathi, T., Sudha, P.N., Anil, S., 2017. Removal of the heavy metal ion chromiuim(VI) using Chitosan and Alginate nanocomposites. Int. J. Biol. Macromol. 104, 1459–1468.
Gokul, V., Mahajan, A., 2017. Femina, Preparation and characterization of micro porous activated carbon prepared from Prosopis Juliflora with chemical and thermal activation. Res. J. Eng. Sci. 6, 5–11.
Gokulan, R., Ganesh Prabhu, G., Jegan, J., 2019. A novel sorbent Ulva lactuca-derived biochar for remediation Remazol brilliant orange 3R in packed column. Water Environ. Res. 91, 642–649.
Han, R., Wang, Y., Zhaoc, X., Wanga, Y., Xieb, F., Cheng, J., Tang, M., 2009. Adsorption of methylene blue by phoenix tree leaf powder in a fixed-bed column: experiments and prediction of breakthrough curves. Desalination 245, 284–297.
Hassan, A.F., Abdel-Mohsen, A.M., Fouda, M.M.G., 2014. Comparative study of calcium alginate, activated carbon, and their composite beads on methylene blue adsorption. Carbohydr. Polym. 102, 192–198.
Ho, Y.S., Chiang, C.C., 2001. Sorption studies of acid dye by mixed sorbents. Adsorption 7, 139–147.
Ho, Y.S., McKay, G., 1998. Sorption of dye from aqueous solution by peat. Chem. Eng. J. 70, 115–124.
Ho, Y.S., McKay, G., 2003. Sorption of dyes and copper ions onto biosorbents. Process Biochem. 38, 1047–1061.
Ho, Y.S., Mckay, G., Wase, D.A.J., Foster, C.F., 2000. Study on the sorption of divalent metal ions onto peat. Adsorpt. Sci. Technol. 18, 639–650.
Jain, C.K., Sharma, M.K., 2002. Adsorption of cadmium on bed sediments of River Hindon: adsorption models and kinetics. Water Air Soil Pollut. 137, 1–19.
Kannan, N., Sundaram, M.M., 2001. Kinetics and mechanism of removal of methylene blue by adsorption on various carbons-A comparative study Kinetics. Dyes Pigments 51, 25–40.
Kumar, M., Tamilarasan, R., 2013. Kinetics and equilibrium studies on the removal of victoria blue using Prosopis juliflora-modified carbon/Zn/alginate polymer composite beads. J. Chem. Eng. Data 58, 517–527.
Lagergren, S., 1898. About the theory of so called adsorption of soluble substances. K. - Sven. Vetenskapsakademiens Handl. 24, 1–39.
Langmuir, I., 1918. Adsorption of gases on plane surfaces of glass, mica and platinum. The J. American Chemical society 40, 1361–1403.
Li, Y., Du, Q., Liu, T., Sun, J., Wang, Y., Wu, S., Wang, Z., Xia, Y., Xia, L., 2013. Methylene blue adsorption on graphene oxide/calcium alginate composites. Carbohydr. Polym. 95, 501–507.
Markandeya, SinghA., Shukla, S.P., Mohan, D., Singh, N.B., Bhargava, D.S., Shukla, R., Pandey, G., Yadav, V.P., Kisku, G.C., 2015. Adsorptive capacity of sawdust for the adsorption of MB dye and designing of two-stage batch adsorber. Cogent Environ. Sci. 1, 1–16.
Markovska, L., Meshko, V., Noveski, V., Marinovski, M., 2001. Solid diffusion control of the adsorption of basic dyes onto granular activated carbon and natural zeolite in fixed bed columns. J. Serb. Chem. Soc. 66, 463–475.
Namasivayam, C., Prabha, D., Kumutha, M., 1988. Removal of direct red and acid-brilliant blue by adsorption on to banana pith. Bioresour. Technol. 64 (1), 77–79.
Nasrullah, A., Bhat, A.H., Naeem, A., Isa, M.H., Danish, M., 2018. High surface area mesoporous activated carbon-alginate beads for efficient removal of methylene blue. Int. J. Biol. Macromol. 107, 1792–1799.
Ofomaja, A.E., Naidoo, E.B., Modose, S.J., 2010. Dynamic studies and pseudo-second order modeling of copper (II) biosorption onto pine cone powder. Desalination 251, 112–122.
Pathania, D., Sharma, S., Singh, P., 2017. Removal of methylene blue by adsorption onto activated carbon developed from Ficus carica bast. Arabian. J. Chem. 10, 1445–1451.
Plazinslic, W., 2010. Applicability of the film-diffusion model for description of the adsorption kinetics at the solid/solution interfaces. Appl. Surf. Sci. 256 (2010), 5157–5163.
Rahimi, M., 2013. Removal of methylene blue from wastewater by adsorption onto ZnCl2 activated corn husk carbon equilibrium studies. J. Chem. 2013, 1–6.
Rebah, Ben, Faouzi, Siddeeg, Eldin, Saif, 2017. Cactus an eco-friendly material for wastewater treatment: a review. J. Mater. Environ. Sci. 8, 1770–1782.
Saber-Samandari, S.S., Samaneh, Saeed, Joneidi Yekta, H., Mohseni, M., 2016. Adsorption of anionic and cationic dyes from aqueous solution using gelatin-based magnetic nanocomposite beads comprising carboxylic acid functionalized carbon nanotube. Chem. Eng. J. 308, 1133–1144.
Safa, Y., Bhatti, H.N., 2011. Adsorptive removal of direct textile dyes by low cost agricultural waste: application of factorial design analysis. Chem. Eng. J. 161, 35–41.
Said, A.E.A., Aly, A.A.M., Goda, M.N., 2020. Adsorptive remediation of Congo red dye in aqueous solutions using acid pretreated sugarcane bagasse. J. Polym. Environ. 28, 1129–1137.
Salleh, M.A.M., Mahmoud, D.K., Karim, W.A., Idris, A., 2011. Cationic and anionic dye adsorption by agricultural solid wastes: a comprehensive review. Desalination 280, 1–13.
Savova, D., Petrov, N., Yardim, M.F., Ekinci, E., Budinova, T., Razvigorova, M., 2003. The influence of the texture and surface properties of carbon adsorbents obtained from biomass products on the adsorption of manganese ions from aqueous solution. Carbon 41, 1897–1903.
Singh, D., Sowmya, V., Abinandan, S., 2018. Removal of malachite green dye by mangifera indica seed kernel powder. J. Inst. Eng. India Ser. A. 99, 103–111.
Singha, S., Sarkar, U., 2015. Analysis of the dynamics of a packed column using semi-empirical models: case studies with the removal of hexavalent chromium from effluent wastewater. Kor. J. Chem. Eng. 32, 20–29.
Sivaraj, R., Namasivayam, C., Kadirvelu, K., 2001. Orange peel as an adsorbent in the removal of acid Violet 17 (acid dye) from aqueous solutions. Waste Manag. 21, 105–110.
Tseng, R.L., Wu, F.C., Juang, R.S., 2003. Liquid-phase adsorption of dyes and phenols using pinewood-based activated carbons. Carbon 41, 487–495.
Vijayaraghavan, K., Thilakavathi, M., Palanivelu, K., Velan, M., 2005. Continuous sorption of copper and cobalt by crab shell particles in a packed column. Environ. Technol. 26, 267–276.
Weber, W.J., Morris, J.C., 1963a. Kinetics of adsorption on carbon from solution. J. Sanity. Eng. Div. Am. Soc. Civ. Eng. 89, 31–59.
Weber, W.J., Morris, J.C., 1963b. Kinetics of adsorption on carbon from solution. J. Sanit. Eng. Div. Am. Soc. Civ. Eng. 89, 31–60.
Wu, F.C., Tseng, R.L., Juang, R.S., 2002. Adsorption of dyes and humic acid from water using chitosan-encapsulated activated carbon. J. Appl. Chem. Biotechnol. 77, 1269–1279.
Xie, T., Reddy, K.R., Wang, C., Yargicoglu, E., Spokas, K., 2015. Characteristics and

applications of biochar for environmental remediation: a review. Crit. Rev. Environ. Sci. Technol. 45, 939–969.

Yang, H., Sheng, K., 2012. Characterization of biochar properties affected by different pyrolysis temperatures using visible-near-infrared spectroscopy. International Scholarly Research Network ISRN Spectroscopy 712837, 1–7. https://doi.org/10.5402/2012/712837.

Zhang, F., Lan, J., Zhao, Z., Yang, Y., Tan, R., Song, W., 2012. Removal of heavy metal ions from aqueous solution using Fe3O4–SiO2-poly (1, 2-diaminobenzene) core–shell sub-micron particles. J. colloid Interference science. 387, 205–212.